

## Can Mueller-Regge models describe inclusive data consistently?\*

Stephen S. Pinsky

*High Energy Physics Division, Argonne National Laboratory, Argonne, Illinois 60439  
and Ohio State University, Columbus, Ohio 43210*

Gerald H. Thomas

*High Energy Physics Division, Argonne National Laboratory, Argonne, Illinois 60439  
(Received 24 October 1973)*

An attempt is made to understand, both phenomenologically and theoretically, the details of inclusive processes. A complete phenomenological analysis of all inclusive pion data in the central region is presented (in the context of the Mueller-Regge picture with three trajectories  $P$ ,  $\rho$ , and  $f$ ). Particular attention is paid to the constraints of charge conjugation and the approach to scaling. All the data are found to fit quite well, including two-body correlations, which have been in considerable variance in previous treatments. One consequence is the prediction that  $\pi\pi$  correlations scale from above. At NAL energies, the nonscaling part is found to be large. The constraint on the couplings ( $\gamma$ ) imposed by charge conservation,  $\gamma^{PP} = 4(\gamma^P \rho)^2 / (\alpha_P - \alpha_\rho)$ , is satisfied. In addition, a number of couplings are found to be approximately exchange-degenerate. Based upon the phenomenological indications, we try to construct the simplest possible Mueller-Regge model with three trajectories obeying the constraints of charge conservation and with an exchange-degenerate  $\rho$  and  $f$ . It is found that it is not possible to consistently construct such a model without adding additional physical mechanisms such as narrow-width resonances. Nevertheless, a model satisfying the above constraints without an exchange-degenerate  $\rho$  and  $f$  can be constructed and has many interesting properties that are borne out by the data. In the calculation of this model, extensive use is made of the recently proven equivalence of the Mueller-Regge and multi-peripheral models.

### I. INTRODUCTION

Now that the initial results from the CERN ISR and the NAL have been circulated, and the most obvious conclusions drawn,<sup>1</sup> it becomes important to attempt a more detailed analysis of the vast amount of data available. A particularly fruitful approach towards these new data has been the use of Mueller-Regge ideas.<sup>2</sup> For our purposes, this means the explanation of inclusive distributions by Regge poles through the use of generalized optical theorems. So far these ideas have been applied to data in the crudest form. One of the most important defects has been that charge and isospin conservation have not been imposed, nor has the positivity of exclusive prong cross sections been ensured.<sup>3</sup> We believe that an important next step is to construct more realistic models. In pursuit of this goal, we shall first compile the relevant data into a form which is useful to any Mueller-Regge analysis. Then we shall discuss the simplest realistic model for these data, and the problems it encounters.

The phenomenological analysis is complete and self-contained, and more detailed than any other to date.<sup>3</sup> Particular attention is paid to the approach to scaling in both one-particle and two-particle correlations, and constraints of charge conservation. It is shown that the relevant two-

body correlations scale from above, and that  $R$  [see Eq. (2.17)] is a slowly scaling quantity which accounts for the unsatisfactory results in other analyses which fail to consider nonscaling terms. The experimental equality of various charge and  $\gamma$  correlations is discussed and shown to be a general Mueller result even for the leading nonscaling terms. The relevant couplings in the Mueller-Regge model (MRM) are extracted from the data wherever possible.

That we encounter problems in our attempt to construct the simplest realistic model is not trivial, but a deep problem of the theory. Nevertheless, the problems we find are in some sense obvious. One of the main advantages of the Mueller-Regge approach is that we deal directly with the Pomeron and secondary trajectories expected to dominate the total and inclusive cross sections. Important properties, such as early scaling and, more generally, the approach to scaling, can be treated directly.<sup>4</sup> Well-studied problems having to do with the Pomeron singularity<sup>5</sup> are not in evidence. The difficulties become apparent when one attempts to include internal quantum numbers in the discussion, and go beyond those statements made in simple models involving only scalar mesons. The attempt to understand the rate at which various cross sections scale has been unsuccessful. This problem of course is closely tied to the

question of exoticity and exchange degeneracy in two-body scattering. Indeed, the connection between the Mueller-Regge approach and the old multiperipheral approach has recently been made more precise.<sup>6</sup> Specifically, for the one-dimensional version of the  $N$ -channel multiperipheral model (MPM) where the dependence on transverse momenta has been integrated out, an exact equivalence has been found with the one-dimensional MRM. This equivalence is expected to be true in some sense for more general multi-Regge and Mueller-Regge models, though the proof of this more general statement is not complete. The general connection, which is suggested, emphasizes that every problem encountered in the MPM can be expected and, in fact, must reappear in the MRM. Consequently, the problems we uncover in trying to construct a charge-conserving MRM are precisely those found by previous authors<sup>7</sup> trying to construct a *realistic* MPM. It is in this sense that our difficulties are obvious, but nevertheless important to point out.

The specific problem we deal with in this paper is that of constructing a MRM which conserves charge and has a set of leading trajectories which roughly agree with experiment. The highest trajectory corresponds to the Pomeron ( $\alpha = 1$ ), while the lower ones are approximated by a  $\rho$  and  $f$  trajectory with exchange-degenerate intercept at  $\alpha = \frac{1}{2}$ . As we shall discuss, these summarize the bulk of present inclusive data. A charge-conserving MRM with these three trajectories must satisfy an infinite set of sum rules,<sup>8</sup> and there may or may not be a solution. In fact our result is that it is not possible to find a simple solution. Nevertheless, a non-exchange-degenerate  $\rho$  and  $f$  solution does exist, and it displays many of the features found in the phenomenological analysis.

The simplest solution to the problem is one in which only three poles exist in the MRM. Such a model is equivalent to a three-channel MPM: The output poles of the MPM are just the Mueller-Regge poles  $P$ ,  $\rho$ ,  $f$ . The construction we require, therefore, is a charge-conserving MRM having exchange-degenerate secondaries. It is well known in some circles that this problem, as stated, has no solution,<sup>7</sup> nor is the solution to a simple generalization of this problem known. Although the leading output pole has  $I=0$ , the highest secondary has  $I=1$ , and an intercept higher than the mixed  $I=0, 2$  pole. Reasonable values for the input trajectories force the  $I=0, 2$  pole to be below  $\alpha=0$ .

One possible solution to this problem that we discuss here involves converting the  $\rho$  and  $f$  trajectories into narrow-width resonances in the "dual" channels.<sup>9</sup> Then it is possible to make

them act as if they were a set of exchange-degenerate trajectories. This model agrees quite well with experiment for integrated quantities. Of course, for unintegrated quantities, there will be a  $\delta$ -function resonance whose interpretation is somewhat dubious. Another possible solution appears to be to introduce a  $Pf$  cut contribution into the input (at  $\approx \frac{3}{4}$ ) in addition to the  $I=0$  ( $PP$ ),  $I=1$  ( $\rho\rho$ ), and  $I=0$  ( $ff$ ) cuts. This is being investigated, although it too may have well-studied difficulties.

Section II contains a summary of the relevant phenomenology, and Sec. III contains a calculation of a charge-conserving MRM. The calculation is formulated in multiperipheral language, and several details are given for completeness. Suggestions of where to go from here are given in the Conclusion, along with a discussion of how inclusive densities should be normalized (whether by  $\sigma_{\text{tot}}$ ,  $\sigma_{\text{inel}}$ , or otherwise).

## II. PHENOMENOLOGY

The data of interest to us, which are currently available, are single- and two-particle inclusive distributions of secondaries, charge multiplicity distributions, and semi-inclusive distributions such as the mean number of neutrals vs prong number.<sup>1</sup> They have in common the property that they characterize the bulk of the inelastic cross section at lab momenta above  $\approx 100$  GeV/ $c$ . In the current nomenclature, we study the "central region" processes, ignoring those processes which are dominant in "fragmentation" or "triple-Regge" regions. In what follows, we make the reasonable assumption that the dependence of transverse momenta can be integrated over, without losing any essential physics other than the known fact that mean transverse momenta are small. The differential behavior of cross sections is studied as a function of the longitudinal momenta; for these variables we use the center-of-mass rapidities,  $y_i$ , defined as

$$y = \frac{1}{2} \ln \frac{E + p_{\parallel}}{E - p_{\parallel}},$$

for a particle of c.m. energy  $E$  and c.m. longitudinal momentum  $p_{\parallel}$ .

With these brief remarks which limit our inquiry, we turn now to the task of summarizing the data in the Mueller-Regge language. This summary will then be used as a guide for constructing specific Mueller-Regge models.

At the present level of accuracy of data, it appears possible to explain the gross features of  $pp$  and  $\pi p$  reactions yielding pions inclusively in a simple Mueller picture, which includes a Pomeron

with intercept approximately unity and two normal-parity, positive- $G$ -parity trajectories  $\rho$  and  $f$ , each with intercept approximately  $\frac{1}{2}$ . The approximate equality of  $\rho$  and  $f$  intercepts is needed to account for total-cross-section data.

We realize, of course, that as data become more accurate, the simple Mueller picture may have to be modified. Nevertheless, we believe that, as in two-body scattering, those modifications need not change our simple qualitative understanding in terms of a few simple Regge poles.

#### A. Single-particle distributions

For the process  $ab \rightarrow cX$  (where  $c$  is the observed particle and  $X$  represents the unobserved states), Fig. 1 shows the various contributions (to order  $s^{-1/4}$ ) expected in our simple Mueller-Regge picture. The single-particle density, normalized by  $\sigma_{\text{tot}}$ , not  $\sigma_{\text{inel}}$  (this choice will be discussed in detail in the conclusion),

$$\rho_c^{ab}(y) \equiv \frac{1}{\sigma_{\text{tot}}} \frac{d\sigma}{dy}(ab \rightarrow cX), \quad (2.1)$$

receives five contributions, one for each diagram in Fig. 1:

$$\begin{aligned} \rho_c^{ab}(y) = & \gamma^{PP} + e^{-Y/4} \left[ e^{y/L} \left( \frac{\delta_a^f}{\delta_b^f} \gamma_c^{Pf} + \frac{\delta_a^\rho}{\delta_b^\rho} \gamma_c^{P\rho} \right) \right. \\ & \left. + e^{-y/L} \left( \frac{\delta_a^f}{\delta_b^f} \gamma_c^{fP} + \frac{\delta_a^\rho}{\delta_b^\rho} \gamma_c^{\rho P} \right) \right]. \end{aligned} \quad (2.2)$$

Here  $Y = \ln(s/s_0)$  is the total "volume" of rapidity available, the  $\delta_i^j$  are the "end" MRM couplings (isospin symmetry requires  $\bar{\delta}_b^\rho = -\delta_b^\rho$ ), the  $\gamma_k^{ij}$  are the Regge-Regge-particle-particle couplings of the center vertex,  $\gamma^{PP}$  is the asymptotic height of the plateau, and

$$\frac{1}{L} = \alpha_P - \alpha_M \quad (2.3)$$

is the difference in intercept of the Pomeron and meson ( $\rho, f$ ) trajectories. In this notation, the total cross section for  $ab$  scattering is, asymptotically,

$$\sigma_{\text{tot}}^{ab} = \delta_a^P \delta_b^P. \quad (2.4)$$

For the present analysis, a constant limit for  $\sigma_{\text{tot}}$  is assumed since the Pomeron is assumed to be a simple pole. A rising cross section, requiring a complicated Pomeron singularity,<sup>10</sup> would necessarily change some of the analysis presented here.

If we consider  $\pi$  production, then isospin conservation requires the following relationships between the Mueller couplings  $\gamma_k^{ij}$ :

$$\begin{aligned} \gamma_-^{P\rho} &= -\gamma_-^{\rho P} = -\gamma_+^{P\rho} = \gamma_+^{\rho P} \equiv -\gamma^{P\rho}, \\ \gamma_-^{Pf} &= \gamma_-^{fP} = \gamma_+^{Pf} = \gamma_+^{fP} = \gamma_0^{fP} = \gamma_0^{Pf} \equiv \gamma^{Pf}, \\ \gamma_0^{\rho P} &= \gamma_0^{P\rho} = 0. \end{aligned} \quad (2.5)$$

Empirical information about individual couplings can then be obtained from a consideration of data on  $p\bar{p} \rightarrow \pi^\pm X$ ,  $\pi^+p \rightarrow \pi^\pm X$ , and  $\pi^-p \rightarrow \pi^\pm X$  at  $y=0$ . Available data<sup>11</sup> on these reactions are given in Figs. 2 and 3, plotted vs  $e^{-Y/4}$ . For consistency with the simple model used here, we want the single-particle densities to have the form

$$\rho_c^{ab}(0) = \gamma^{PP} + h_c^{ab} e^{-Y/4}$$

for each reaction. The results for  $h_c^{ab}$  using "eyeball fits" to the data are given in Table I. The MRM couplings can then be obtained by taking particular combinations of cross sections at  $y=0$ :

$$\gamma^{P\rho} \frac{\delta_\rho^\rho}{\delta_P^\rho} = -\frac{1}{4}(h_{\pi^+}^{\pi^+p} - h_{\pi^-}^{\pi^+p} + h_{\pi^+}^{\pi^-p} - h_{\pi^-}^{\pi^-p}) \quad (2.6a)$$

$$= -\frac{1}{4}(h_{\pi^+}^{\rho\rho} - h_{\pi^-}^{\rho\rho}), \quad (2.6b)$$

$$\begin{aligned} \gamma^{P\rho} \frac{\delta_\rho^\rho}{\delta_{\pi^+}^\rho} &= -\frac{1}{4}(h_{\pi^+}^{\pi^+p} - h_{\pi^-}^{\pi^+p} - h_{\pi^+}^{\pi^-p} + h_{\pi^-}^{\pi^-p}) \\ &= -\gamma^{P\rho} \frac{\delta_{\pi^-}^\rho}{\delta_{\pi^+}^\rho}, \end{aligned} \quad (2.6c)$$

$$\gamma^{Pf} \frac{\delta_f^f}{\delta_P^f} = \frac{1}{4}(h_{\pi^+}^{\rho\rho} + h_{\pi^-}^{\rho\rho}), \quad (2.6d)$$

$$\gamma^{Pf} \frac{\delta_{\pi^+}^f}{\delta_{\pi^+}^f} = \frac{1}{2}(h_{\pi^+}^{\pi^+p} + h_{\pi^-}^{\pi^+p}) - \frac{1}{4}(h_{\pi^+}^{\rho\rho} + h_{\pi^-}^{\rho\rho}) \quad (2.6e)$$

$$= \gamma^{Pf} \frac{\delta_{\pi^-}^f}{\delta_{\pi^+}^f}. \quad (2.6f)$$

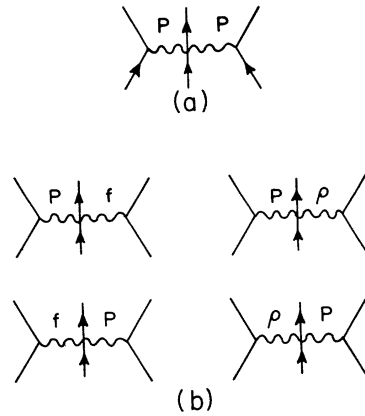


FIG. 1. (a) The leading (scaling) MRM amplitude. (b) The nonleading corrections to order  $s^{-1/4}$  assuming only pion production from  $p\bar{p}$  and  $\pi p$  reactions.

TABLE I. Exclusive and inclusive couplings. The exclusive couplings  $\delta_i^j$  are taken from Ref. 12; the inclusive couplings  $h_c^{ab}$  are taken from fits to data  $\rho = \gamma^{PP} + h_c^{ab} e^{-Y/4}$  in Figs. 2 and 3. The fits determine  $\gamma^{PP} = 0.75 \pm 0.1$ ; Eqs. (2.6a)–(2.6f) determine  $\gamma^{P\rho} = -0.4 \pm 0.2$ ,  $-0.5 \pm 0.2$ ,  $-0.46 \pm 0.06$ ,  $\gamma^{Pf} = -0.44 \pm 0.04$ ,  $-0.34 \pm 0.1$ ,  $-0.4 \pm 0.1$ , respectively.

	$X = \text{total}$	$X = \pi^+ X'$	$X = \pi^- X'$
$pp \rightarrow X$	$\left\{ \begin{array}{l} \delta_b^f / \delta_b^P = 1.0 \\ \delta_b^\rho / \delta_b^P = 0.2 \end{array} \right\}$	$h_{\pi^+}^{pp} = -0.69 \pm 0.08$	$h_{\pi^-}^{pp} = -1.1 \pm 0.1$
$\pi^+ p \rightarrow X$	$\left\{ \begin{array}{l} \delta_{\pi^+}^f / \delta_{\pi^+}^P = 0.8 \\ \delta_{\pi^+}^\rho / \delta_{\pi^+}^P = 0.8 \end{array} \right\}$	$h_{\pi^+}^{\pi^+ p} = -0.27 \pm 0.1$	$h_{\pi^-}^{\pi^+ p} = -1.2 \pm 0.05$
$\pi^- p \rightarrow X$	$\left\{ \begin{array}{l} \delta_{\pi^-}^f / \delta_{\pi^-}^P = 0.8 \\ \delta_{\pi^-}^\rho / \delta_{\pi^-}^P = -0.8 \end{array} \right\}$	$h_{\pi^+}^{\pi^- p} = -1.1 \pm 0.1$	$h_{\pi^-}^{\pi^- p} = -0.5 \pm 0.1$

The external ratios  $\delta_i^j / \delta_i^P$  are known from two-body reactions<sup>12</sup> (Table I), leaving three free parameters,  $\gamma^{P\rho}$ ,  $\gamma^{Pf}$ , and  $\gamma^{PP}$ , to be determined from the single-particle inclusive data. The separate determinations are consistent with<sup>3</sup>

$$\begin{aligned} \gamma^{PP} &\cong 0.75 \pm 0.1, \\ \gamma^{P\rho} &= \gamma_+^{P\rho} \cong -0.45 \pm 0.1, \\ \gamma^{Pf} &= \gamma_+^{Pf} \cong -0.40 \pm 0.1, \end{aligned} \quad (2.7)$$

showing that the  $\rho$  and  $f$  have approximately exchange-degenerate couplings

$$\gamma^{Pf} \cong \gamma^{P\rho} \equiv \gamma^{PM}$$

within the errors of our determination (see caption of Table I). Note that for  $\pi^-$  production  $\rho$  and  $f$  couplings have opposite signs, whereas for  $\pi^+$  production the couplings have the same sign. It is worthwhile pointing out that the signs of  $\gamma^{P\rho}$  and  $\gamma^{Pf}$  depend upon the convention that for  $b = p$  and  $\pi^+$   $\delta_b^a > 0$  ( $\delta_b^a < 0$ ) and the empirical determinations that  $\gamma^{P\rho} \delta_b^\rho / \delta_b^P$  and  $\gamma^{Pf} \delta_b^f / \delta_b^P$  are negative. Other than the above sign conventions, we know of no fundamental reason why  $\gamma_c^{ab}$  must be positive.<sup>13</sup> In the multiperipheral models we discuss later, we show that  $\gamma^{PM}$  can be negative in certain cases.

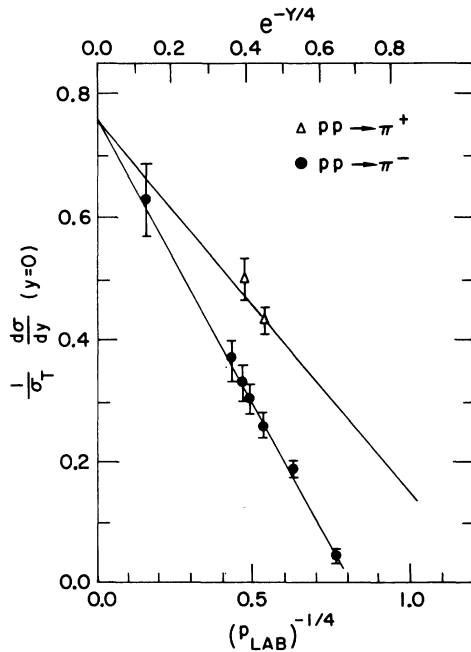


FIG. 2. The approach to scaling of the  $pp \rightarrow \pi X$  single-particle density  $(1/\sigma_T) d\sigma/dy$  at  $y = 0$ . The straight lines are hand-drawn fits through the data (see Ref. 11).

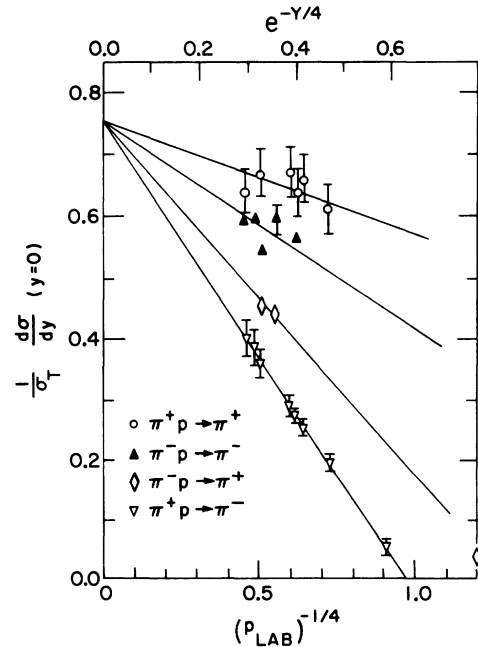


FIG. 3. As in Fig. 2 for  $\pi p \rightarrow \pi X$ .

## B. Two-particle correlations

The number of possible MRM graphs for the two-particle inclusive density is 27 in our three-pole phenomenology. Not all contribute, of course, to order  $s^{-1/4}$ , and some are identically canceled when computing the two-particle correlation function

$$C_{c_1 c_2}^{ab}(y_1, y_2) = \frac{1}{\sigma_{\text{tot}}} \frac{d^2 \sigma}{dy_1 dy_2} - \left( \frac{1}{\sigma_{\text{tot}}} \frac{d\sigma}{dy_1} \right) \left( \frac{1}{\sigma_{\text{tot}}} \frac{d\sigma}{dy_2} \right) \quad (2.8)$$

for the process  $ab \rightarrow c_1 c_2 X$ . For  $pp$  and  $\pi p$  reactions producing pions, to order  $s^{-1/4}$  we can again, as in the single-particle density case, restrict attention to only  $\rho$ - and  $f$ -meson exchanges. Then all MRM graphs having a Pomeron in the center rung cancel in  $C_{c_1 c_2}^{ab}$ , leaving ten graphs having a Pomeron at one end and  $\rho$  and  $f$  exchanges in the other rungs. In addition, four terms from the product of single-particle densities survive. The net result of all these graphs is

$$C_{c_1 c_2}^{ab}(y_1, y_2 | Y) = \exp\left(\frac{y_1 - y_2}{L}\right) \gamma_{c_1}^{Pf} \gamma_{c_2}^{Pf} (1 - \tau_1 \tau_2) \\ + e^{-Y/4} \left\{ -\gamma_{c_1}^{Pf} \gamma_{c_2}^{PP} e^{y_1/L} \left[ \frac{\delta_b^f}{\delta_b^P} \left( 1 - \frac{\gamma_{c_2}^{ff} - \tau_1 \gamma_{c_2}^{f\rho}}{\gamma_{c_2}^{PP}} \right) - \frac{\delta_b^\rho}{\delta_b^P} \left( \tau_1 - \frac{\gamma_{c_2}^{f\rho} + \tau_1 \gamma_{c_2}^{\rho\rho}}{\gamma_{c_2}^{PP}} \right) \right] \right. \\ \left. - \gamma_{c_2}^{Pf} \gamma_{c_1}^{PP} e^{-y_2/L} \left[ \frac{\delta_a^f}{\delta_a^P} \left( 1 - \frac{\gamma_{c_1}^{ff} - \tau_2 \gamma_{c_1}^{f\rho}}{\gamma_{c_1}^{PP}} \right) - \frac{\delta_a^\rho}{\delta_a^P} \left( \tau_2 - \frac{\gamma_{c_1}^{f\rho} + \tau_2 \gamma_{c_1}^{\rho\rho}}{\gamma_{c_1}^{PP}} \right) \right] \right\}$$

for  $y_2 \geq y_1$  and where  $\tau_i = \gamma_{c_i}^{P\rho} / \gamma_{c_i}^{Pf}$ . For charged pion production, the correlations  $C_{c_1 c_2}^{ab}$  so computed depend upon three new parameters  $\gamma^{f\rho} \equiv \gamma_+^{f\rho}$ ,  $\gamma^{ff} \equiv \gamma_+^{ff}$ , and  $\gamma^{\rho\rho} \equiv \gamma_+^{\rho\rho}$ . Ultimately, data on  $C_{c_1 c_2}^{ab}$  will give the magnitudes of these quantities.

We now proceed to use the available data on  $pp \rightarrow \pi\pi X$  to obtain some rough information on the meson-meson couplings, as well as to check some of the qualitative predictions of the MRM scheme for the correlation functions. We shall assume in the following the approximate exchange degeneracy  $\gamma^{Pf} \cong \gamma^{P\rho} \cong \gamma^{PM}$  found above. One immediate consequence is the vanishing of  $C_{++}$  and  $C_{--}$  (i.e., correlations for  $ab \rightarrow \pi^+ \pi^+ X$  and  $ab \rightarrow \pi^- \pi^- X$ , respectively) asymptotically. To order  $s^{-1/4}$  further statements can be made. The sum of  $C_{++}$  and  $C_{--}$ ,

$$\frac{1}{2}(C_{++} + C_{--}) = -\gamma^{PM}(\gamma^{PP} + \gamma^{f\rho} - \gamma^{ff}) \\ \times \left( \frac{\delta_b^f}{\delta_b^P} e^{y_1/L} + \frac{\delta_a^f}{\delta_a^P} e^{-y_2/L} \right) e^{-Y/4}, \\ y_2 \geq y_1 \quad (2.9a)$$

has  $P$  and  $f$  end couplings only. Experimental information on  $pp \rightarrow \pi^+ \pi^+ X$  at 205 GeV/c indicates that<sup>14</sup>

$$C_{++}(0, 0) \cong 0.36 \pm 0.04, \quad (2.10a)$$

$$C_{--}(0, 0) \cong 0.20 \pm 0.02. \quad (2.10b)$$

At the same energy, the MRM gives

$$\frac{1}{2}[C_{++}(0, 0) + C_{--}(0, 0)] = +0.14 \left( 1 + \frac{\gamma^{f\rho} - \gamma^{ff}}{\gamma^{PP}} \right), \quad (2.11a)$$

compared with 0.28 from the data. The data are too preliminary for us to draw a strong conclusion, but the present indication is that

$$\gamma^{f\rho} - \gamma^{ff} \cong \gamma^{PP}. \quad (2.12a)$$

It is worth noting the prediction that  $\frac{1}{2}(C_{++} + C_{--})$  decreases to zero like  $s^{-1/4}$ . Present data do not yet have sufficient accuracy over a wide enough range of energy to allow a reliable determination of this nonscaling.

Next, we consider the difference between  $C_{++}$  and  $C_{--}$ ,

$$\frac{1}{2}(C_{++} - C_{--}) = \gamma^{PM}(\gamma^{PP} - \gamma^{f\rho} - \gamma^{\rho\rho}) \\ \times \left( \frac{\delta_b^\rho}{\delta_b^P} e^{y_1/L} + \frac{\delta_a^\rho}{\delta_a^P} e^{-y_2/L} \right) e^{-Y/4}, \\ y_2 \geq y_1 \quad (2.9b)$$

which has only  $P$  and  $\rho$  end couplings. For  $y_1 \approx y_2 \approx 0$ , the fact that  $\delta_{\pi^\pm}^\rho$  and  $\delta_b^\rho$  couplings differ by sizable amounts leads to the ratios (at the same  $Y$ )

$$(pp) : (\pi^+ p) : (\pi^- p) = 0.4 : 1 : -0.6$$

for  $\frac{1}{2}(C_{++} - C_{--})$ . At 205 GeV/c, for  $pp$  reactions, this difference is

$$\frac{1}{2}(C_{++} - C_{--}) \cong -0.03 \left(1 - \frac{\gamma^{f\rho} + \gamma^{\rho\rho}}{\gamma^{PP}}\right), \quad (2.11b)$$

compared with the experimental value<sup>14</sup> of +0.08. We certainly obtain a qualitative understanding of

$$C_{+-} = 2(\gamma^{PM})^2 e^{-|y_2 - y_1|/L} - \gamma^{PM}(\gamma^{PP} - \gamma^{f\rho} - \gamma^{ff}) \left(\frac{\delta_b^f}{\delta_b^P} e^{y_1/L} + \frac{\delta_a^f}{\delta_a^P} e^{-y_2/L}\right) e^{-Y/4} \\ + \gamma^{PM}(\gamma^{PP} + \gamma^{f\rho} - \gamma^{\rho\rho}) \left(\frac{\delta_b^P}{\delta_b^f} e^{y_1/L} - \frac{\delta_a^P}{\delta_a^f} e^{-y_2/L}\right) e^{-Y/4}, \quad y_2 \geq y_1 \quad (2.9c)$$

has the approximate maximum<sup>14</sup>

$$C_{+-}(0, 0) \sim 0.50 \pm 0.02 \quad (2.10c)$$

at 205 GeV/c for  $pp \rightarrow \pi^+ \pi^- X$ . Compare this with the MRM value

$$C_{+-}(0, 0) \cong 0.36 + 0.14 \left(1 - \frac{\gamma^{f\rho} + \gamma^{ff}}{\gamma^{PP}}\right). \quad (2.11c)$$

Equivalently, one can compare the experimental value of

$$C_{\text{ch ch}}(0, 0) \cong 2C_{+-} + C_{++} + C_{--} \\ \cong 1.56 \pm 0.15$$

with the model

$$C_{\text{ch ch}}(0, 0) = 0.72 + 0.56 \left(1 - \frac{\gamma^{ff}}{\gamma^{PP}}\right).$$

The value of 0.5 for  $C_{+-}$  indicates

$$\gamma^{f\rho} \cong -\gamma^{ff}, \quad (2.12b)$$

which yields, coupled with Eq. (2.12a), the additional result

$$\gamma^{ff} \cong -\frac{1}{2}\gamma^{PP}. \quad (2.12c)$$

Finally, we analyze some preliminary CERN ISR data on charge-charge and charge- $\gamma$  correlations:

$$C_{\text{ch } \gamma} \cong 2C_{+0} + 2C_{-0}, \quad (2.13)$$

$$C_{\gamma\gamma} \cong 4C_{00}, \quad (2.14)$$

where the subscript 0 refers to  $\pi^0$  production. In obtaining these formulas, we assume that all  $\gamma$ 's come from  $\pi^0$  decay, and that for  $C_{\gamma\gamma}$  the  $\gamma$ 's come from different  $\pi^0$ 's. Moreover, we assume the  $\gamma$ - $\gamma$  and  $\gamma$ -charge correlation lengths to be about  $L$ . In the MRM to order  $s^{-1/4}$ , we find

$$C_{\text{ch ch}}^{ab}(y_1, y_2) = C_{\text{ch } \gamma}^{ab}(y_1, y_2) \\ = C_{\gamma\gamma}^{ab}(y_1, y_2), \quad (2.15)$$

where for  $y_2 \geq y_1$

the smallness of the difference. At this point, the data are not accurate enough for us to check the sign, and hence we obtain no information about  $\gamma^{f\rho} + \gamma^{\rho\rho}$ .

Experimentally, the largest correlation,

$$C_{\gamma\gamma} = 4(\gamma^{Pf})^2 e^{-|y_2 - y_1|/L} \\ - 4\gamma^{Pf}\gamma^{PP} \left(1 - \frac{\gamma^{ff}}{\gamma^{PP}}\right) \left(\frac{\delta_b^f}{\delta_b^P} e^{y_1/L} + \frac{\delta_a^f}{\delta_a^P} e^{-y_2/L}\right) \\ \times e^{-Y/4} \quad (2.16)$$

without assuming exchange degeneracy.

This exact equality (2.15) is probably a reflection of the isospin structure of the four-to-four Mueller amplitude, and can probably be derived on more general grounds. ISR data<sup>15</sup> (Fig. 4) indicate that these relations are well satisfied.

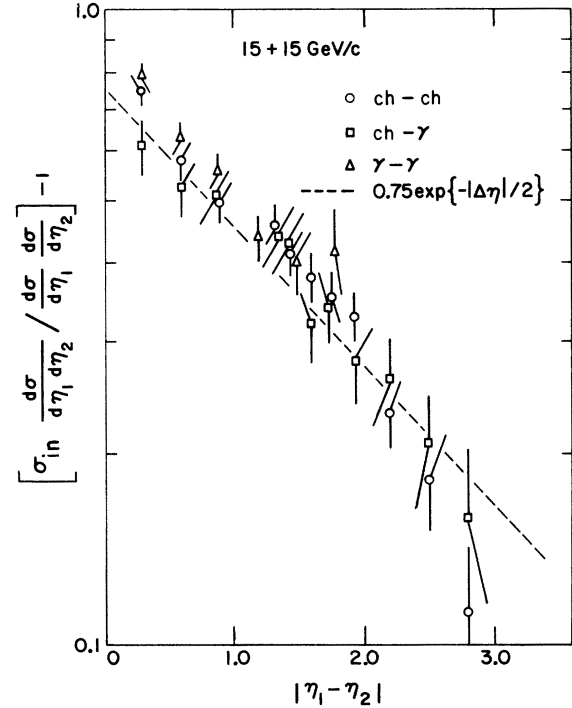


FIG. 4. The normalized correlation data (2.17) for charged-charged, charged- $\gamma$ , and  $\gamma$ - $\gamma$  taken at the CERN ISR (Ref. 15) at colliding-beam energies of 15 GeV/c upon 15 GeV/c. The correlations are plotted against  $\Delta\eta = |\eta_1 - \eta_2|$ , where  $\eta = \ln \tan(\theta_{\text{c.m.}}/2)$ .

(Note that one has to first convert the data plotted,

$$R^{\text{inel}} = \sigma_{\text{inel}} \frac{d\sigma/dy_1 dy_2}{(d\sigma/dy_1)(d\sigma/dy_2)} - 1, \quad (2.17)$$

to the correlation function

$$C(y_1, y_2) = \left[ (R^{\text{inel}} + 1) \frac{\sigma_{\text{tot}}}{\sigma_{\text{inel}}} - 1 \right] \rho(y_1) \rho(y_2). \quad (2.18)$$

The relation holds since  $\frac{1}{2}[\rho_+(0) + \rho_-(0)]$  and  $\rho_0(0)$  are approximately equal at ISR energies and hence  $\rho_{\text{ch}} \cong \rho_{\gamma}$ .

It is important to note that the quantity  $R$  has a large nonscaling part. The reason for this is that the numerator scales from above while the denominator scales from below, and the effects add. As a result, we can expect a large variation for NAL energies to ISR energies. With the parameters we have found

$$R_{\text{inel}}^{\text{ch ch}}(0, 0) = 0.9 \pm 0.3 \text{ at NAL (200 GeV/c),}$$

$$R_{\text{inel}}^{\text{ch ch}}(0, 0) = 0.5 \pm 0.15 \text{ at ISR (1500 GeV/c).}$$

The experiments unfortunately have large relative normalization uncertainties, making comparison impossible at this time.

Certainly the above results for  $\gamma^{ff}$ ,  $\gamma^{f\rho}$ , and (when the data improve)  $\gamma^{\rho\rho}$  are very preliminary. Nevertheless, they indicate the trend of present data and provide a basis for discussing the MRM. The qualitative conclusions are the following:

- (1)  $\gamma^{Pf} \approx \gamma^{P\rho}$  and  $\gamma^{ff} \approx -\gamma^{f\rho}$ ; namely, the  $\rho$  and  $f$  are exchange-degenerate in coupling.
- (2)  $\gamma^{ff} = -\frac{1}{2}\gamma^{PP}$ ; the Pomeron and  $f$  have different couplings, although we do find  $\gamma^{fP} \approx \gamma^{ff}$ .
- (3) The value  $\gamma^{PP} \approx \frac{3}{4}$ , which gives  $\langle n_{\pi^-} \rangle$  per inelastic collision increasing like  $\frac{4}{3}\gamma^{PP} \ln s \cong \ln s$ , is in rough agreement with available data.
- (4) There are appreciable nonscaling contributions to  $C_{++}$ ,  $C_{+-}$ , and  $C_{--}$ ; this nonscaling behavior can be tested in a way analogous to that of the nonscaling behavior in the single-particle distribution.
- (5) Data on charge- $\gamma$  correlations give tentative support for the MRM picture obtained from studying  $C_{\pm\pm}$  and  $C_{+-}$ .
- (6) There is an exact equality to order  $s^{-1/4}$ ,

$$C_{\text{ch ch}} = C_{\text{ch } \gamma} = C_{\gamma \gamma},$$

which holds over the entire pionization region if the connection between  $\gamma$ 's and  $\pi$ 's is made in a simple intuitive way.

### C. Charge-conserving MRM

Before calculating an explicit model, we check first some general constraints on the MRM due to charge conservation. For studying these constraints it is sufficient to consider only integrated

inclusive quantities, or equivalently the moments of the multiplicity distribution. We define

$$I(x, y, z) = \sum \sigma(n_+, n_-, n_0) x^{n_+} y^{n_-} z^{n_0} \quad (2.19)$$

in terms of the cross section for producing  $n_+$  positive,  $n_-$  negative, and  $n_0$  neutral particles. The infinite set of charge-conserving sum rules are equivalent to the requirement<sup>16</sup>

$$I(x, y, z) = x^q I(1, xy, z), \quad (2.20)$$

where  $q$  is the charge of the initial state ( $pp$  scattering has  $q=2$ ). It will also be convenient to use the Mueller-type moments  $f_{ijk}$  defined by

$$I(x, y, z) = \exp \left[ \sum_{i,j,k=0}^{\infty} \frac{f_{ijk}^{+-0}}{i!j!k!} (x-1)^i (y-1)^j (z-1)^k \right]. \quad (2.21)$$

For brevity, we use  $f_{ijk} \equiv f_{ijk}^{+-0}$  whenever no confusion results. At NAL energies, available data indicate that three-particle and higher moments are zero (i.e., small).<sup>17</sup> Although there may be reason to believe that this situation may change at asymptotic energies,<sup>18</sup> these statements can be useful approximations in the NAL-ISR energy regime. In what follows, we shall assume the statements to be true.

With the above assumption, the charge constraint Eq. (2.20) implies that  $I(x, y, z)$  has the form

$$I(x, y, z) = x^q \exp[(xy-1)f_{010}]; \quad (2.22)$$

we ignore for now neutral-particle production ( $z=1$ ). This form, in turn, implies that  $f_{010} = f_{110}$ , i.e.,

$$\langle n_- \rangle = \langle n_+ n_- \rangle - \langle n_+ \rangle \langle n_- \rangle. \quad (2.23)$$

If we use the leading behavior of the MRM integrated over  $y_1$  and  $y_2$ , (2.23) implies

$$\gamma^{PP} = 2[(\gamma^{Pf})^2 + (\gamma^{P\rho})^2] L. \quad (2.24a)$$

From (2.22) we see that the absence of three-body and higher correlations requires  $f_{020}$  and  $f_{200}$  to be absent, i.e.,

$$\langle n_-(n_- - 1) \rangle - \langle n_- \rangle^2 \approx 0. \quad (2.25)$$

This is equivalent to the statement that  $\sigma_{n_-}$  is a Poisson distribution. Again using the leading behavior of the MRM for  $f_{020}$ , we find

$$2L[(\gamma^{Pf})^2 - (\gamma^{P\rho})^2] = 0,$$

implying that

$$(\gamma_{\pm}^{Pf})^2 = (\gamma_{\pm}^{P\rho})^2, \quad (2.26)$$

which is satisfied approximately by the data. Thus charge conservation and the fact the three-body and higher correlations appear to be small over the present range of energies imply exchange de-

generacy in the square of the coupling. In addition, we have the constraint of charge conservation<sup>19</sup> from (2.24a) and (2.26):

$$\gamma^{PP} = 4L(\gamma^{P\rho})^2. \quad (2.24b)$$

This result, however, is more general than the discussion here and is derived from applying our MRM to the exact relation [see Eq. (3.37)]

$$f_{010} = f_{1,1,0} - f_{0,2,0}.$$

If we use  $\gamma^{PP} \cong 0.75$ , (2.24b) requires  $|\gamma^{PM}| \cong 0.31$ , in approximate agreement with  $\gamma^{PM} \cong -0.42$  as determined from analyzing  $\rho(y)$ .

Additional constraints result from considering neutral-particle production. The generating function has the charge-conserving form

$$I(x, y, z) = x^q \exp[(xy - 1)f_{010} + (z - 1)f_{001} + \frac{1}{2}(z - 1)^2 f_{002} + (xy - 1)(z - 1)f_{011}] \quad (2.27)$$

under the assumption of no correlations higher than two-body. (Note that, in fact, a three-body correlation,  $f_{111}$ , is introduced; we ignore this contribution.) Since pions are the predominant type of particle produced, we assume in addition  $f_{010} \approx f_{001}$ :

$$\langle n_- \rangle \approx \langle n_+ \rangle \approx \langle n_0 \rangle. \quad (2.28)$$

With these assumptions, we can compute the average number of neutral particles vs number of produced negative particles. The general expression for this quantity is

$$\langle n_0 \rangle_- = \sum_{r=0}^{n_-} \frac{\sigma_{n_- - r}}{\sigma_{n_-}} \frac{F_r}{r!}, \quad (2.29a)$$

where

$$F_r = \sum_{k=r}^{\infty} f_{0k1} \frac{(-1)^{k-r}}{(k-r)!} \quad (2.29b)$$

and  $\sigma_{n_-}$  is the cross section for negative particles which we found to be Poisson,

$$\sigma_{n_-} = \frac{(f_{010})^{n_-}}{n_-!} e^{-f_{010}}, \quad (2.30)$$

and therefore

$$\langle n_0 \rangle_- = f_{001} - f_{011} + \frac{f_{011}}{f_{010}} n_-. \quad (2.31)$$

Equation (2.24b) implies that  $f_{011}/f_{010} \rightarrow \frac{1}{2}$  since asymptotically  $C_{\pm 0} = \frac{1}{2}C_{+-}$  and the integral of  $C_{+-}$  is  $\langle n_- \rangle$  by Eq. (2.23). The result is

$$\langle n_0 \rangle_- = \frac{1}{2}(f_{010} + n_-), \quad (2.32a)$$

which is consistent with available data.<sup>20</sup> The MRM fit gives asymptotically the ratio

$$\frac{f_{011}}{f_{010}} \approx \frac{4(\gamma^{Pf})^2}{\gamma^{PP}} = 1.0; \quad (2.32b)$$

this leads to

$$\langle n_0 \rangle_- = 1.0n_-, \quad (2.32c)$$

which is also consistent with the data. Note that this shows the degree of accuracy to which Eq. (2.24b) has been checked, and emphasizes the crudeness of our analysis.

It is important to note that Eq. (2.32b) involves  $\gamma^{Pf}$ , while the charge constraint (2.24b) only involves  $\gamma^{P\rho}$ . Therefore,  $\langle n_0 \rangle_-$  can be used as a check on the exchange degeneracy of the  $\rho$  and  $f$  coupling. Since  $\gamma^{Pf}$  comes into (2.32b) squared, it is quite sensitive. A 40% breaking of exchange degeneracy, for example, would allow  $\langle n_0 \rangle_- = n_-$ , a result which has been argued for previously in the literature,<sup>18,20</sup> as well as allowing (2.24b) to be satisfied.

### III. A MODEL

As formulated in the Introduction, we wish to construct a charge-conserving Mueller-Regge model (MRM) with three singularities corresponding to the Pomeron  $P$  and the secondary exchanges  $\rho$  and  $f$ . We emphasize that the MRM does not automatically give exclusive cross sections which conserve charge [Eq. (2.24b) is necessary but not sufficient], nor are the cross sections necessarily positive. A trivial example is the elastic cross section

$$\sigma_{el}(s) = \sigma_{tot}(s) \sum_{n=0}^{\infty} (-)^n \rho_n(s),$$

which is a sum over all  $n$ -particle inclusive cross sections  $\sigma_{tot} \rho_n$ . Since the terms alternate in sign, the positivity of  $\sigma_{el}$  is not guaranteed. Similar statements can be made about charge conservation. Therefore, it cannot be taken for granted that the model of Sec. II as it stands will yield results consistent with exclusive data. Nevertheless, it would be extremely satisfactory to have a fairly simple model which agreed with the trend of both inclusive and exclusive data. To this end we subject the three-pole model of Sec. II to certain minimal requirements needed to describe exclusive data.

The plan of this section is to start with a three-channel MPM in which charge and positivity are ensured for all choices of couplings and trajectories. By a recently proved equivalence,<sup>6</sup> any charge-conserving MRM giving positive cross sections is identical to some MPM. Our assumptions on the MPM correspond to charge symmetry rather than complete isospin conservation. After some algebraic manipulations, we show that  $n_0$



reasonable MRM of the form we envisioned in Sec. II can be constructed in the three-channel formulation. Since charge must be rigorously conserved, we then suggest that a simple improvement may be to include resonances in the model. Such a modification would necessarily change the interpretation of the peak in  $C_2(\Delta y)$  from evidence of low-subenergy Regge behavior to evidence for a resonance enhancement. The advantage of such an addition would be to keep the Regge interpretation of inclusive distributions at large subenergies without violating charge conservation or exclusive positivity.

#### A. Calculation of the MRM from the MPM

The most general three-channel MPM, in a one-dimensional approximation (integrating out transverse momentum), has the form<sup>21</sup>

$$\sigma_n(Y) = e^{-Y} \int dy_1 \cdots dy_n \bar{D}^T F(y_1) G F(y_2 - y_1) \cdots \times G F(Y - y_n) D \quad (3.1)$$

for the cross section for producing  $n$  particles. The notation<sup>6</sup> is that the external ( $D$  and  $\bar{D}$ ) and internal ( $G$ ) couplings, as well as the propagator  $F$ , are  $3 \times 3$  matrices. In general, the propagator  $F(x)$  is diagonal, and has the form

$$F(x) = \begin{pmatrix} e^{l_1 x} & 0 & 0 \\ 0 & e^{l_2 x} & 0 \\ 0 & 0 & e^{l_3 x} \end{pmatrix}, \quad (3.2)$$

where  $l_i = 2\alpha_i - 1$  is related to the position of the input Regge pole. Through unitarity, the quantity  $l_i$  is the position in the  $J$  plane of the resulting cut in the absorptive part of the elastic amplitude due to the Regge exchange in the production amplitude. We ignore cuts due to interference terms where  $l = \alpha + \bar{\alpha} - 1$ .

The form of the coupling matrices depends upon the basis. In a charge basis, where rows and columns are labeled by 0, +, and - charge exchanged, the coupling matrices to produce 0,  $\pm$  units of charge are

$$G_+ = \begin{pmatrix} 0 & 0 & \sqrt{2} B \\ \sqrt{2} B & 0 & 0 \\ 0 & 0 & 0 \end{pmatrix} = G_+^T, \quad (3.3)$$

$$G_0 = \begin{pmatrix} A & 0 & 0 \\ 0 & C & 0 \\ 0 & 0 & C \end{pmatrix}, \quad (3.4)$$

where by convention we have charge flowing to the right. To keep track of the amount of produced charge, we write

$$G = xG_+ + yG_- + zG_0 \quad (3.5)$$

so that  $x$ ,  $y$ , and  $z$  generate +, -, and 0 units of charge in (3.1). In this same basis, the external couplings are

$$D = \begin{pmatrix} z d_{11} & y d_{12} & x d_{12} \\ x \sqrt{2} d_{21} & z \sqrt{2} d_{22} & 0 \\ y \sqrt{2} d_{21} & 0 & z \sqrt{2} d_{22} \end{pmatrix}, \quad (3.6)$$

$$\bar{D}^T = \begin{pmatrix} z d_{11} & y \sqrt{2} d_{21} & x \sqrt{2} d_{21} \\ x d_{12} & z \sqrt{2} d_{22} & 0 \\ y d_{12} & 0 & z \sqrt{2} d_{22} \end{pmatrix}. \quad (3.7)$$

The rule for obtaining a particular cross section  $\sigma_{ab}$  from (3.1) is to take the matrix element  $(\bar{D}^T \cdots D)_{a\bar{b}}$ . For example, the ++ cross section is the 23 element, while the +- cross section is the 22 element, etc.

In the charge basis, the form of (3.3) and (3.4) ensures charge conservation and leads to the charge constraints in the MRM. The requirement that  $A, B, C, d_{ij} \geq 0$  ensures the positivity of all cross sections. We must have additionally that

$$l_2 = l_3, \quad (3.8)$$

i.e.,  $\alpha_+ = \alpha_-$ . With these constraints, the model is specified (up to certain arbitrary parameters), and we can turn to the question of rewriting the model in the Mueller-Regge form.

It has been shown in Ref. 6 that the change of (3.1) to the MRM is accomplished by the orthogonal transformation  $S$  which diagonalizes  $(L + G_1)$ , where  $(L)_{ij} = \delta_{ij} l_i$  and  $G_1 = G(x=1, y=1, z=1)$ ; that is,  $S$  satisfies

$$S^T (L + G_1) S = \Lambda, \quad (3.9)$$

$$S^T S = I, \quad (3.10)$$

where  $\Lambda = \lambda_i \delta_{ij}$  is the diagonal matrix of the output poles,  $\lambda_i = \alpha_i^{\text{out}}$ .

This is a straightforward calculation by standard techniques. However, experience and some physical insight help to reduce the calculational difficulties. Since the Mueller model has only neutral exchange, the symmetric and antisymmetric combinations of the + and - charges tend to be a more natural basis. As a result of this,  $S$  will have the simple form

$$S = \begin{pmatrix} 1 & 0 & 0 \\ 0 & 1/\sqrt{2} & -1/\sqrt{2} \\ 0 & 1/\sqrt{2} & 1/\sqrt{2} \end{pmatrix} \begin{pmatrix} \cos\theta & -\sin\theta & 0 \\ \sin\theta & \cos\theta & 0 \\ 0 & 0 & 1 \end{pmatrix}.$$

We find after straightforward manipulations

$$\lambda_{1,2} = \frac{1}{2}(A + l_1 + C + l_2) \pm \left\{ \left[ \frac{1}{2}(A + l_1 - C - l_2) \right]^2 + 4B^2 \right\}^{1/2}, \quad (3.11)$$

$$\lambda_3 = C + l_2, \quad (3.12)$$

$$\tan 2\theta = \frac{4B}{A + l_1 - C - l_2}. \quad (3.13)$$

From positivity of  $A$ ,  $B$ , and  $C$ , several constraints follow immediately. First we rewrite the expressions for (3.11)–(3.13), so that  $A$ ,  $B$ ,  $C$ , and  $\theta$  are expressed solely in terms of the input and output singularities  $l_i$  and  $\lambda_i$ :

$$A = \lambda_1 + \lambda_2 - \lambda_3 - l_1 > 0, \quad (3.14)$$

$$C = \lambda_3 - l_2 > 0, \quad (3.15)$$

$$B = \frac{1}{2}[(\lambda_1 - \lambda_3)(\lambda_3 - \lambda_2)]^{1/2} > 0, \quad (3.16)$$

$$\tan\theta = -\left(\frac{\lambda_3 - \lambda_2}{\lambda_1 - \lambda_3}\right)^{1/2}. \quad (3.17)$$

In order that some amplitude for charged particles exist, we see that  $\lambda_3 \neq \lambda_2$  and  $\lambda_1 \neq \lambda_3$ . Moreover, if we want the Pomeron ( $\lambda_1$ ) to be leading, we have

$$\Gamma_+ = \Gamma_-^T = \begin{pmatrix} B \sin 2\theta & B \cos 2\theta & B \cos \theta \\ B \cos 2\theta & -B \sin 2\theta & -B \sin \theta \\ -B \cos \theta & B \sin \theta & 0 \end{pmatrix}, \quad (3.21a)$$

$$\Gamma_0 = \begin{pmatrix} \frac{1}{2}(A+C) + \frac{1}{2}(A-C)\cos 2\theta & -\frac{1}{2}(A-C)\sin 2\theta & 0 \\ -\frac{1}{2}(A-C)\sin 2\theta & \frac{1}{2}(A+C) - \frac{1}{2}(A-C)\cos 2\theta & 0 \\ 0 & 0 & C \end{pmatrix}, \quad (3.21b)$$

$$\Delta = \begin{pmatrix} z d_{11} \cos\theta + (x+y)d_{21} \sin\theta & y d_{12} \cos\theta + z d_{22} \sin\theta & x d_{12} \cos\theta + z d_{22} \sin\theta \\ -z d_{11} \sin\theta + (x+y)d_{21} \cos\theta & -y d_{12} \sin\theta + z d_{22} \cos\theta & -x d_{12} \sin\theta + z d_{22} \cos\theta \\ -(x-y)d_{21} & -z d_{22} & z d_{22} \end{pmatrix}. \quad (3.21c)$$

Various properties of these matrices will be used below.

#### B. Qualitative features of the internal couplings $\gamma_k^{ij}$

Now let us be more explicit about the calculation of inclusive distributions and the total cross section. Step one is to compute the Laplace transform

from (3.16)

$$\lambda_3 > \lambda_2, \quad (3.18)$$

a very important constraint expressing the results that the antisymmetric ( $I=1$ ) output trajectory is higher than the symmetric ( $I=0, 2$ ) output trajectory. We believe this result to be more general than the simple model considered here. *It is because of this result that an exchange-degenerate solution cannot be found in the simple framework considered here.* Note that the constraints (3.14), (3.15) require simply that

$$2\alpha_1^{\text{in}} - 1 < \alpha_1^{\text{out}}, \quad (3.19)$$

$$2\alpha_2^{\text{in}} - 1 < \alpha_1^{\text{out}},$$

showing the well-known result that the Pomeron singularity cannot be generated by an input singularity at unity.

It is appropriate at this time to mention the results of the calculation for the inclusive coupling matrices

$$\begin{aligned} \Gamma_i &= S^T G_i S, \\ \Gamma &= (x-1)\Gamma_+ + (y-1)\Gamma_- + (z-1)\Gamma_0, \\ \Delta &= S^T D, \end{aligned} \quad (3.20)$$

$$\bar{\Delta}^T = \bar{D}^T S = \Delta^T(x \leftrightarrow y).$$

After some uninteresting algebra, we obtain

$$\begin{aligned} Q_n(J) &\equiv \int_0^\infty dY e^{-(J-1)Y} \sigma_n(Y) \\ &= \bar{D}^T F(J) [GF(J)]^n D, \end{aligned} \quad (3.22)$$

where  $F(J)$  is the Laplace transform of  $F(x)$ . Step

two is to use the result of Ref. 6 that

$$(\Phi(J))_{ij} = \delta_{ij} \frac{1}{J - \lambda_i}, \quad (3.25)$$

$$Q = \sum_{n=0}^{\infty} Q_n(J) = \sum_{n=0}^{\infty} P_n(J), \quad (3.23)$$

where

$$P_n(J) = \bar{\Delta}^T \Phi(J) [\Gamma \Phi(J)]^n \Delta, \quad (3.24)$$

and  $\Delta$ ,  $\bar{\Delta}$ , and  $\Gamma$  are defined above (3.20). The interpretation of  $P_n(J)$  is that  $P_0$  is the transform of the total cross section,  $P_1$  the transform of the single-particle rate, etc. For example, the (transform of the) total cross section of  $\pm\pm$  scattering is

$$P_0(+\pm) = \frac{(d_{12} \cos\theta + d_{22} \sin\theta)^2}{J - \lambda_1} + \frac{(-d_{12} \sin\theta + d_{22} \cos\theta)^2}{J - \lambda_2} \mp \frac{d_{22}^2}{J - \lambda_3}, \quad (3.26)$$

showing the standard result that the  $\rho(I=1)$  contribution to  $pp$  scattering, for example, is negative, whereas the contribution to  $p\bar{p}$  scattering is positive. The two symmetric contributions behave as expected, by not changing signs between  $ab$  and  $a\bar{b}$  scattering and by being positive. As a further example, the single-particle  $\pm$  production in  $++$  scattering is

$$\begin{aligned} P_1^{\pm}(++) &= (\bar{\Delta}^T \Phi \Gamma_{\pm} \Phi \Delta)_{23} \\ &= \frac{B \sin 2\theta (d_{12} \cos\theta + d_{22} \sin\theta)^2}{(J - \lambda_1)(J - \lambda_1)} + \frac{2B \cos 2\theta (d_{12} \cos\theta + d_{22} \sin\theta)(-d_{12} \sin\theta + d_{22} \cos\theta)}{(J - \lambda_1)(J - \lambda_2)} \\ &\quad \pm \frac{2B \cos\theta (d_{12} \cos\theta + d_{22} \sin\theta) d_{22}}{(J - \lambda_1)(J - \lambda_3)} + \text{lower terms}. \end{aligned} \quad (3.27)$$

In a similar way, higher inclusive cross sections can be calculated. Note that the three trajectories behave formally like a  $P$ ,  $f$ , and  $\rho$  trajectory, and so the calculations can be done as in Sec. II without the formal matrix manipulations used here.

Denoting the matrix elements of  $\Gamma_{\pm}$  by  $\gamma^{ij}$  and those of  $\Gamma_0$  by  $\gamma_0^{ij}$ , and using the suggestive notation  $i, j = P, f, \rho$ , we now compute the MRM internal couplings. It will be convenient to introduce the following additional notation:

$$\beta = \lambda_1 - \lambda_3 = \alpha_P^{\text{out}} - \alpha_{\rho}^{\text{out}} > 0, \quad (3.28a)$$

$$g_0 = \lambda_3 - \lambda_2 = \alpha_{\rho}^{\text{out}} - \alpha_f^{\text{out}} > 0, \quad (3.28b)$$

$$f = \frac{\lambda_3 - l_2}{\lambda_1 - \lambda_3} > 0, \quad (3.28c)$$

$$\epsilon = \frac{\lambda_1 + \lambda_2 - \lambda_3 - l_1}{\lambda_3 - \lambda_2} + \frac{\lambda_3 - l_2}{\lambda_1 - \lambda_3} > f. \quad (3.28d)$$

The elements of  $\Gamma_{+,0}$  are obtained by using (3.21), where in the above notation

$$A = g_0(\epsilon - f),$$

$$B = \frac{1}{2}(\beta g_0)^{1/2},$$

$$C = \beta f,$$

$$\sin\theta = \pm \left( \frac{g_0}{g_0 + \beta} \right)^{1/2},$$

$$\cos\theta = \pm \left( \frac{\beta}{g_0 + \beta} \right)^{1/2}.$$

The sign ambiguity for  $\sin\theta$  and  $\cos\theta$  is tentatively resolved by adopting by convention the negative sign. The results for the internal coupling are

$$\gamma^{PP} = -\gamma^{ff} = \frac{\beta g_0}{\beta + g_0}, \quad (3.29a)$$

$$\gamma_0^{PP} = \epsilon \frac{\beta g_0}{\beta + g_0}, \quad \gamma_0^{ff} = \frac{g_0^2(\epsilon - f) + \beta^2 f}{\beta + g_0}, \quad (3.29b)$$

$$\gamma^{Pf} = \gamma^{fP} = \frac{1}{2}(\beta g_0)^{1/2} \frac{\beta - g_0}{\beta + g_0}, \quad (3.29c)$$

$$\gamma_0^{Pf} = \gamma_0^{fP} = (\beta g_0)^{1/2} \frac{\beta f - g_0(\epsilon - f)}{\beta + g_0}, \quad (3.29d)$$

$$\gamma^{P\rho} = -\gamma^{\rho P} = -\frac{1}{2}\beta \left( \frac{g_0}{\beta + g_0} \right)^{1/2}, \quad (3.29e)$$

$$\gamma_0^{P\rho} = -\gamma_0^{\rho P} = 0, \quad (3.29f)$$

$$\gamma^{f\rho} = -\gamma^{\rho f} = \frac{1}{2}g_0 \left( \frac{\beta}{\beta + g_0} \right)^{1/2}, \quad (3.29g)$$

$$\gamma_0^{f\rho} = -\gamma_0^{\rho f} = 0, \quad (3.29h)$$

$$\gamma^{\rho\rho} = 0, \quad (3.29i)$$

$$\gamma_0^{\rho\rho} = \beta f. \quad (3.29j)$$

We are now in a position to compare certain qualitative features of the above charge-conserving MRM internal couplings with those couplings found in Sec. II using available data. The charge sum rule (2.24b) is seen to hold exactly in the form involving only the  $\rho$  coupling,

$$\gamma^{PP} = \frac{4(\gamma^{PP})^2}{\alpha_P - \alpha_\rho} \quad (3.30)$$

A second result to note is that the relative signs (with our convention for  $\sin\theta$  and  $\cos\theta$ ) are in agreement with the signs of the empirically derived couplings. Namely, with  $\gamma^{PP}$  positive, both  $\gamma^{Pf}$  and  $\gamma^{P\rho}$  can be negative,  $\gamma^{ff}$  and  $\gamma^{f\rho}$  have opposite signs, and  $\gamma^{f\rho}$  is positive. Moreover,  $\gamma^{ff} = -\gamma^{P\rho}$  is within a factor 2 of the empirical result  $\gamma^{ff} \cong -\frac{1}{2}\gamma^{PP}$ . Finally, the couplings that vanish are  $\gamma^{PP}$ ,  $\gamma_0^{f\rho}$ , and  $\gamma_0^{P\rho}$ . Isospin required  $\gamma_0^{ff}$  and  $\gamma_0^{P\rho}$  to vanish, and  $\gamma^{PP}$  is a coupling that could not be determined.

Of course, in determining the couplings, we have not enforced all the isospin constraints necessary to ensure realistic  $P$ ,  $f$ , and  $\rho$  trajectories. For example, the  $P$  should couple equally to  $\pi^\pm$  and  $\pi^0$  so that  $\gamma_0^{PP} = \gamma^{PP}$ . This would require  $\epsilon = 1$ , implying that  $f < 1$  since  $A = g_0(1-f) > 0$ . If we take  $\alpha_1^{\text{out}} = 1$ , the implication is then

$$\alpha_3^{\text{out}} < \alpha_2^{\text{in}}, \quad (3.31)$$

i.e., the asymmetric output pole must lie lower than the input charged trajectories.

Isospin also requires that  $\gamma_0^{Pf} = \gamma^{Pf}$ , which with  $\epsilon = 1$  implies that  $f = \frac{1}{2}$ . This is necessary to ensure the equality of  $C_{\text{ch ch}}$ ,  $C_{\text{ch } \gamma}$ , and  $C_{\gamma\gamma}$  observed experimentally (see Sec. II). If we continue, however, and try to enforce  $\gamma_0^{ff} = \gamma^{ff}$ , we arrive at a contradiction, namely that  $g_0 = -\beta$ , whereas both  $g_0$  and  $\beta$  are strictly positive. The result is therefore that the three poles cannot represent two pure  $I = 0$  states and one  $I = 1$  state. In what follows, we will assume only that one channel is  $I = 0$ , one channel is  $I = 1$ , and the lower symmetric channel is a mixture of  $I = 0$  and 2. The only results we might want to enforce would be  $\epsilon = 1$ , because  $P$  should be pure  $I = 0$ , and  $f = \frac{1}{2}$ , since  $C_{\text{ch ch}}$ ,  $C_{\text{ch } \gamma}$ , and  $C_{\gamma\gamma}$  are empirically equal. Setting  $\epsilon = 1$ ,  $f = \frac{1}{2}$ , and  $\alpha_1^{\text{out}} = 1$ , we then find

$$\begin{aligned} \alpha_2^{\text{in}} &= \frac{3}{4}\alpha_3^{\text{out}} + \frac{1}{4} = 1 - \frac{3}{4}\beta, \\ \alpha_1^{\text{in}} &= 1 - \frac{3}{4}(\alpha_3^{\text{out}} - \alpha_2^{\text{out}}) \\ &= 1 - \frac{3}{4}g_0, \end{aligned}$$

$$\begin{aligned} \alpha_+(xy, z) - \lambda_1 &= -\frac{1}{2}\beta[1 - (z-1)f] - \frac{1}{2}g_0[1 - (z-1)(\epsilon - f)] \\ &+ \left\{ \left( \frac{1}{2}\beta[1 - (z-1)f] - \frac{1}{2}g_0[1 - (z-1)(\epsilon - f)] \right)^2 + xy\beta g_0 \right\}^{1/2}. \end{aligned} \quad (3.34)$$

In terms of this, the cross section for ++ scattering is

$$\sigma(xy, z) = x^2 \text{residue}(xy, z) \exp[\alpha_+(xy, z) - 1] Y, \quad (3.35)$$

showing that  $\alpha_3^{\text{out}}$  and  $\alpha_2^{\text{out}}$  are the only free parameters left in the theory.

A final comment on the couplings is the note that a negative value for  $\gamma^{Pf}$  implies that

$$\alpha_\rho - \alpha_f > \alpha_P - \alpha_\rho$$

[which, if  $\epsilon = 1$ ,  $f = \frac{1}{2}$ , and  $\alpha_1^{\text{out}} = 1$ , implies  $\alpha_2^{\text{in}} > \alpha_1^{\text{in}}$ , i.e., the  $\rho$  must lie further above the  $f$  than the  $P$  lies above the  $\rho$  (recall  $\alpha_\rho > \alpha_f$ ). This result emphasizes once again the defect the model has, namely, it does not allow exchange-degenerate intercepts  $\alpha_\rho = \alpha_f$ . Nevertheless, the model we have constructed may be of some theoretical interest since it is a charge-conserving model, even though the exchange degeneracy we initially sought cannot be realized. For example, the couplings  $\gamma^{ij}$  have some features in common with the data, as is true also for the multiplicity moments as we shall see. Some of these general features may well persist in more complicated models. With this expectation, we proceed to an investigation of the leading behavior of the integrated correlation moments.

### C. Multiplicity moments and the inclusion of resonances

The moments of the multiplicity distribution we obtain in closed form by evaluating the generating function  $Q$  as a function of  $x, y, z$ : Derivatives of  $\ln Q$  with respect to  $x, y, z$  (evaluated at  $x=y=z=1$ ) will yield the moments in question. The evaluation of  $Q$  for our problem can be done explicitly [see (3.22)]:

$$Q = \bar{D}^T F(J) [I - GF(J)]^{-1} D, \quad (3.32)$$

where the leading behavior of the cross section is determined by the position of the leading zero of

$$\det[I - GF(J)] = 0. \quad (3.33)$$

We denote the leading zero by  $J = \alpha_+(xy, z)$ , since charge conservation forces  $Q$  to have the form  $x^q f(xy, z)$ , where  $q$  is the initial charge. Using the notation (3.28) we calculate the position  $\alpha_+$  to be

and asymptotically the first few multiplicity moments

$$f_{klm} \rightarrow \frac{\partial^k}{\partial x^k} \frac{\partial^l}{\partial y^l} \frac{\partial^m}{\partial z^m} \alpha_+(xy, z) Y \quad (3.36)$$

are

$$\langle n_0 \rangle = f_{001} = \epsilon \frac{g_0 \beta}{g_0 + \beta} Y, \quad (3.37a)$$

$$\langle n_{\pm} \rangle = f_{100} = f_{010} = \frac{g_0 \beta}{g_0 + \beta} Y, \quad (3.37b)$$

$$[\langle n_{\pm}(n_{\pm} - 1) \rangle - \langle n_{\pm} \rangle^2] = f_{200} = f_{020} = -2 \frac{g_0^2 \beta^2}{(g_0 + \beta)^3} Y, \quad (3.37c)$$

$$[\langle n_+ n_- \rangle - \langle n_+ \rangle \langle n_- \rangle] = f_{110} = \frac{g_0 \beta (g_0^2 + \beta^2)}{(g_0 + \beta)^3} Y, \quad (3.37d)$$

$$[\langle n_0(n_0 - 1) \rangle - \langle n_0 \rangle^2] = f_{002} = 2 \frac{g_0 \beta (g_0(\epsilon - f) - \beta f)^2}{(g_0 + \beta)^3} Y, \quad (3.37e)$$

$$\begin{aligned} \langle n_0 n_{\pm} \rangle - \langle n_0 \rangle \langle n_{\pm} \rangle &= f_{101} \\ &= f_{011} = \frac{g_0 \beta (g_0 - \beta) [g_0(\epsilon - f) - \beta f]}{(g_0 + \beta)^3} Y, \end{aligned} \quad (3.37f)$$

etc.

The quantities  $f_{110}$ ,  $f_{002}$ , and  $f_{101}$  [(3.37d)–(3.37f)] are measured at ISR energies and found to be positive. More precisely, ISR measurements yield the two-particle correlations for charge-charge, charge- $\gamma$ , and  $\gamma$ - $\gamma$ :

$$\begin{aligned} f_{\text{ch ch}} &\rightarrow (2f_{110} + f_{200} + f_{020}), \\ f_{\text{ch } \gamma} &\rightarrow 2f_{101} + 2f_{011}, \\ f_{\gamma \gamma} &\rightarrow 4f_{002}. \end{aligned} \quad (3.38)$$

All three quantities are approximately equal and positive. Consider for a moment the implication of having  $f_{011} > 0$ ; it implies that

$$(g_0 - \beta) [g_0(\epsilon - f) - \beta f] > 0. \quad (3.39)$$

The two possible choices of parameters are (1)  $g_0/\beta > 1$  and  $g_0/\beta > f/(\epsilon - f)$  or (2)  $g_0/\beta < 1$  and  $g_0/\beta < f/(\epsilon - f)$ . On the one hand, we come closest to exchange degeneracy when  $g_0 < \beta$ , i.e. [from (3.28)],

$$\alpha_2^{\text{out}} > 2\alpha_3^{\text{out}} - \alpha_1^{\text{out}}. \quad (3.40)$$

On the other hand, if the highest secondary ( $\alpha_3^{\text{out}}$ ) is at  $\frac{1}{2}$  and  $\alpha_1^{\text{out}} = 1$  ( $\beta = \frac{1}{2}$ ), then the slope of the mean number of particles  $\langle n_{\pm,0} \rangle / Y < \frac{1}{2}$ ; the maximum slope  $\langle n \rangle / Y$  comes for  $g_0$  large and hence  $g_0 > \beta$ :

$$\alpha_3^{\text{out}} < 2\alpha_2^{\text{out}} - \alpha_1^{\text{out}}. \quad (3.41)$$

The latter may be the most natural solution, emphasizing that  $\alpha_2$ , the  $I=0, 2$  symmetric output secondary, does not represent the  $f$ , but rather  $I=0$  and  $2$  low-lying daughter and exotic trajectories. As shown above, it also ensures that  $\gamma^{Pf}$

[(3.29c)] is negative.

In (3.37c), we see that the second correlation moment for negatives and for positives is less than zero, contrary to the data. In part this is due to the lack of exchange degeneracy in the model. To fake an exchange-degenerate model, we let  $\beta \rightarrow \infty$  so that  $\lambda_2/\lambda_3 \rightarrow 1$ . In this case, the moments (3.37) become

$$f_{001} = \epsilon g_0 Y, \quad (3.42a)$$

$$f_{100} = f_{010} = g_0 Y, \quad (3.42b)$$

$$f_{200} = f_{020} = 0, \quad (3.42c)$$

$$f_{110} = g_0 Y, \quad (3.42d)$$

$$f_{002} = 2g_0 f^2 Y, \quad (3.42e)$$

$$f_{101} = f_{011} = g_0 f Y. \quad (3.42f)$$

All the moments are positive or zero, a situation completely in agreement with data. In fact, the generating function becomes in the limit  $\beta \rightarrow \infty$

$$\alpha_+(xy, z) = g_0 \left[ (z-1)\epsilon + \frac{(xy-1) + (z-1)^2 f^2}{1 - (z-1)f} \right]. \quad (3.43)$$

The physical basis for this model will be discussed elsewhere.<sup>22</sup> For present purposes we note that the limit  $\beta \rightarrow \infty$  is equivalent to a  $\delta$ -function propagator  $F(x)_{ii}$  for  $i=2$  and  $3$ . This would be the case for resonance production using a narrow-width-type approximation. The positive correlations are then due to the presence of resonances, whereas the absence of negative-negative correlations is a constraint of exchange degeneracy and charge conservation. The situation is therefore analogous to two-body scattering where exchange-degeneracy requirements exclude exotic channels.

#### IV. CONCLUSION

We now return to the delicate question of normalization. It is extremely important and goes right to the heart of the central problem in strong interactions today, the nature of the Pomeron. The problem arises when one attempts to have a unitary and self-consistent theory. For example, in the MPM if we have a  $2 \rightarrow n$  amplitude without Pomerons, the model will generate an output Pomeron which can be made to have intercept unity (as dictated by the data). However, if we include this Pomeron in the  $2 \rightarrow n$  amplitude, unitarity will generate an amplitude violating the Froissart bound. As a result of this fundamental problem, an interim procedure called the two-component model has been developed.<sup>23</sup>

In this procedure, the  $2 \rightarrow n$  amplitude is divided into a diffractive part and a nondiffractive part,

each of which is handled separately, and only one of which can be unitarized (the nondiffractive). If one were to use this two-component model to calculate inclusive processes, each component would be normalized according to its appropriate part of the total cross section. Then the two pieces would have to be combined in the appropriate way to get the full inclusive process. To the extent that  $\sigma_{\text{el}}$  is all diffractive, it may be entirely removed from the process as a matter of taste, since it cannot be properly unitarized anyway.

In the phenomenological analysis, however, our objective is not a guide to the construction of a two-component model, but rather a guide to the construction of the ultimate model. Ultimately, it is hoped that we will learn how to unitarize the entire theory and that the effect of the diffractive component will be to renormalize the Pomeron that is generated by the nondiffractive  $2 \rightarrow n$  amplitudes, as well as the other trajectories involved. Furthermore, it is hoped that the leading-pole spectrum will not be changed in any fundamental way. That is to say, the same primary poles will give the major numerical contribution to all physical processes.

With this point of view in mind, we have tried phenomenologically to fit all inclusive data with what are expected to be the most important  $J$ -plane singularities. Since the poles are viewed as the poles of the full amplitude, we must normalize to the total cross section.

The theoretical problems that we are facing now divide into two groups: (1) dynamic and (2) conservation-law constraints. We think it is clear from what we have seen here that the constraints of charge conservation play an important role in the behavior of inclusive cross sections. The constraints of other conservation laws may be equally important.<sup>24</sup> For example, the reason for the slow scaling of  $\bar{p}$  inclusive may be here. The basic isospin properties also need investigation. For ex-

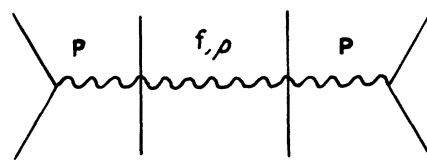


FIG. 5. The scaling MRM graph. The  $\rho$  contribution is absent for ch-ch, ch- $\gamma$ , and  $\gamma$ - $\gamma$  correlations.

ample, the equality of  $C_{\text{ch ch}}$ ,  $C_{\text{ch } \gamma}$ , and  $C_{\gamma \gamma}$  can be understood to leading order as a result of no isospin-2 exchange.<sup>25</sup> The leading contributions to these correlations come from the diagram shown in Fig. 5. The center section of the diagram is identical to  $\pi\pi$  scattering as far as the quantum numbers go, and the three correlation functions receive only  $I=0$  exchange contributions, assuming the absence of  $I=2$ . No doubt, the equality of the nonscaling pieces follows from similar though more complicated arguments.

The dynamical problems that we are facing are, of course, much deeper. The equivalence between the MRM and the MPM tells us that all the problems that beset the MPM bootstrap will reappear here. It is therefore going to be difficult to make progress on the well-studied problem of the Pomeron bootstrap. However, it may be possible to find models which have sufficient complication and freedom to have exchange degeneracy in both the input and output trajectories. As we saw, the  $\delta$ -function model which simulates this property seems to have many nice phenomenological properties.

#### ACKNOWLEDGMENTS

It is a pleasure to acknowledge informative discussions with R. C. Arnold, R. Singer, D. R. Snider, and B. R. Webber. One of us (S.S.P) also acknowledges the hospitality of the High Energy Physics Division at Argonne National Laboratory.

\*Work supported by the U. S. Atomic Energy Commission.

<sup>1</sup>A fairly comprehensive list of references to data and models can be found in D. Sivers and G. H. Thomas, Phys. Rev. D **9**, 208 (1974). Discussion of these data in terms of simple theoretical ideas is presented therein.

<sup>2</sup>A. Mueller, Phys. Rev. D **2**, 2963 (1970). By the term "Mueller-Regge," we mean to consider only Regge-pole exchange in the discontinuity of the  $n$ -to- $n$  forward amplitudes. Cut contributions may well be present but fall outside of the theoretical framework of this paper.

<sup>3</sup>E.g., a Mueller-Regge analysis in the central region

has been done by J. R. Freeman and C. Quigg [Phys. Lett. **B47**, 39 (1973)]. The inclusive couplings (2.7), we find, are in agreement with their results. However, they have not considered consistently the nonasymptotic contributions (of order  $s^{-1/4}$ ) to the two-particle inclusive distribution, nor have they considered the question of positivity of exclusive cross sections or charge-conservation constraints. Since the MRM does not *a priori* obey these constraints, it is necessary to check explicitly whether or not they are satisfied.

<sup>4</sup>Chan Hong-Mo, H. I. Miettinen, D. P. Roy, and P. Hoyer, Phys. Lett. **40B**, 406 (1972).

<sup>5</sup>E.g., violation of the Froissart bound [J. Finkelstein and K. Kajantie, Phys. Lett. **26B**, 305 (1968); Nuovo

- Cimento 56, 659 (1968)]. For a modern approach to these problems, see W. R. Frazer, D. R. Snider, and C.-I Tan, Phys. Rev. D 8, 3180 (1973).
- <sup>6</sup>S. S. Pinsky, D. R. Snider, and G. H. Thomas, Phys. Lett. 47B, 505 (1973).
- <sup>7</sup>H. W. Wyld, Nuovo Cimento 7A, 632 (1972). References to earlier work can be found therein.
- <sup>8</sup>K. J. Biebl and J. Wolf, Phys. Lett. 37B, 197 (1971); C. E. DeTar, D. Z. Freedman, and G. Veneziano, Phys. Rev. D 4, 906 (1971).
- <sup>9</sup>Models of this type are proposed by S. S. Pinsky, D. R. Snider, and G. H. Thomas, Argonne Report No. ANL/HEP-7349 (unpublished).
- <sup>10</sup>See, e.g., proceedings of the Symposium on the Pomeron, 1973, Argonne Report No. ANL/HEP-7327 (unpublished).
- <sup>11</sup>T. Ferbel, Phys. Rev. Lett. 29, 448 (1972); Rochester Report No. COO-3065-41 (unpublished); M. J. Delay *et al.*, in *Experiments on High Energy Particle Collisions—1973*, proceedings of the international conference on new results from experiments on high energy particle collisions, Vanderbilt University, 1973, edited by Robert S. Panvini (A.I.P., New York, 1973), p. 257.
- <sup>12</sup>See, e.g., R. C. Brower, R. N. Cahn, and J. Ellis, Phys. Rev. D 7, 2080 (1973). These authors analyze single- and two-particle inclusive distributions in the fragmentation regions using the Mueller-Regge picture.
- <sup>13</sup>See, however, Ref. 4. Duality considerations may lead to definite signs, although one is then forced to introduce unphysical trajectories to explain the single-particle distributions which scale from below.
- <sup>14</sup>R. Engelmann *et al.*, Argonne Report No. ANL/HEP-7341 (unpublished); and private communication from R. Singer. The data include all charges measured in the plateau region using the  $\ln \tan(\theta_{\text{lab}}/2)$  variable. Ultimately one would want data for charged pions as well. *Note added in proof.* Final data are now available in R. Singer *et al.*, Argonne Reports No. ANL/HEP 7368 and No. ANL/HEP 7369, 1973 (unpublished).
- <sup>15</sup>S. R. Amendolia *et al.*, CERN report, 1973 (unpublished).
- <sup>16</sup>B. R. Webber, Nucl. Phys. B43, 541 (1972).
- <sup>17</sup>See, e.g., W. R. Frazer, R. D. Peccei, S. S. Pinsky, and C.-I Tan, Phys. Rev. D 7, 2647 (1973).
- <sup>18</sup>Calculations in the Bjorken-Feynman-Wilson fluid analog suggest there can be strong three-body and higher correlations when the fluid has critical-point fluctuations. See R. C. Arnold and G. H. Thomas, Phys. Lett. 47B, 371 (1973); G. H. Thomas, Phys. Rev. D 8, 3042 (1973).
- <sup>19</sup>This constraint has been found in specific model calculations [S. S. Pinsky, University of California, Riverside, report, 1972 (unpublished)]. See Ref. 9 of the present paper for revision of this model. For further discussion see R. Amann, M. Blackmon, and K. A. Geer, Phys. Rev. D 9, 1508 (1974).
- <sup>20</sup>The data are discussed by E. L. Berger, D. Horn, and G. H. Thomas, [Phys. Rev. D 7, 1412 (1973)]; see also the analysis by F. T. Dao and J. Whitmore [Phys. Lett. 46B, 252 (1973)].
- <sup>21</sup>C. E. DeTar, Phys. Rev. D 3, 128 (1971).
- <sup>22</sup>Pinsky, Snider, and Thomas, Ref. 9.
- <sup>23</sup>See Ref. 1 for a discussion of various two-component model proposals, as well as for a list of references for such models.
- <sup>24</sup>B. R. Webber, Argonne Report No. ANL/HEP-7348 (unpublished).
- <sup>25</sup>See D. Horn and F. Zachariasen, *Hadron Physics at Very High Energies*, (Benjamin, New York, 1973).